CHEMISTRY
A EUROPEAN JOURNAL

ChemPubSoc
Europe

DOI: 10.1002/chem.201203042

Spiroketal-Based Phosphorus Ligands for Highly Regioselective Hydroformylation of Terminal and Internal Olefins

Xiaofei Jia,[a, b] Zheng Wang,[b] Chungu Xia,*[a] and Kuiling Ding*[b]

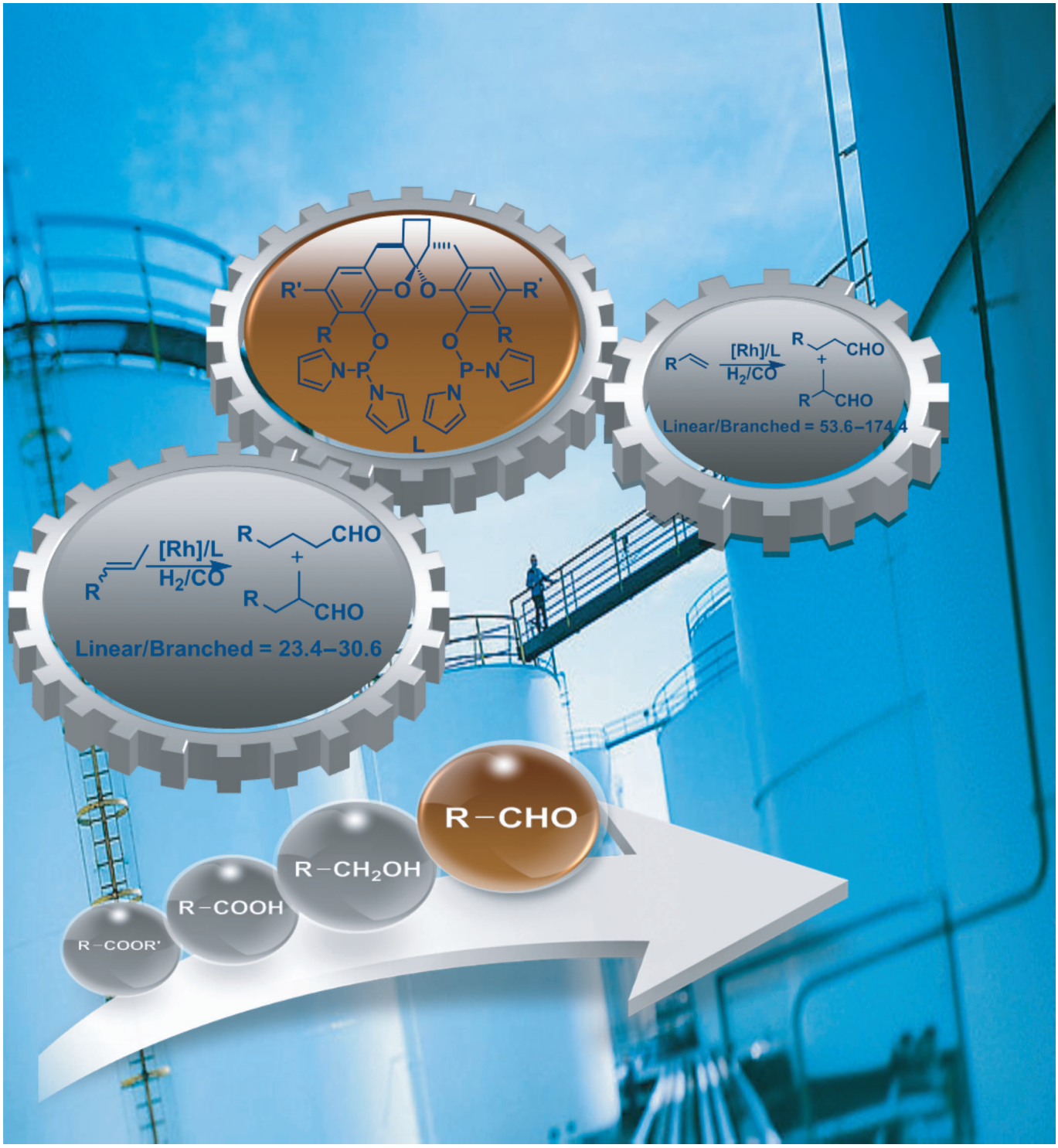

Abstract: A new class of bidentate phosphoramidite ligands, based on a spiroketal backbone, has been developed for the rhodium-catalyzed hydroformylation reactions. A range of short- and long-chain olefins, were found amenable to the protocol, affording high catalytic activity and excellent regioselectivity for the linear aldehydes. Under the optimized reaction conditions, a turnover number (TON) of up to 2.3×10^4 and linear to branched ratio (*l/b*) of up to 174.4 were obtained in the Rh^I-catalyzed hydroformylation of terminal olefins. Remarkably, the catalysts were also found to be efficient in the isomerization–hydroformylation of some internal olefins, to regioselectively afford the linear aldehydes with TON values of up to 2.0×10^4 and *l/b* ratios in the range of 23.4–30.6. X-ray crystallographic analysis revealed the *cis* coordination of the ligand in the precatalyst [Rh(**3d**)(acac)], whereas NMR and IR studies on the catalytically active hydride complex [$HRh(CO)_2$(**3d**)] suggested an eq–eq coordination of the ligand in the species.

Keywords: homogeneous catalysis · hydroformylation · ligands · olefins · regioselectivity · rhodium

Introduction

Rhodium-catalyzed olefin hydroformylation is one of the most important processes of homogeneous catalysis in industry.[1] Several million tons of various aldehydes and their derivatives are produced worldwide per year. A key issue in searching for efficient hydroformylation catalysts is the development of new ligands. Monodentate phosphorus ligands have been most commonly used in commercial hydroformylation processes, but regioselectivity can become a concern in some cases. Over the past several decades, a variety of bisphosphorus ligands[2] have been successfully developed for Rh-catalyzed hydroformylation of olefins (Scheme 1). Despite these efforts, however, the catalytic systems that are efficient and selective for hydroformylation of both terminal olefins and the internal olefins still remain rare so far. Ligands that bear a biaryl scaffold with C_2-symmetry, such as Naphos,[3] Biphephos,[4] DuPont/DSM ligand,[5] pyrrole-based bisphosphoramidite[6] and tetraphosphoramidite,[7] have been reported to show excellent regioselectivities in the hydroformylation of both terminal and internal olefins. Xantphos, with a rigid xanthene structure initiated by van Leeuwen, was shown to be a highly selective hydroformylation catalyst.[8] However, there was still room for improvement in reactivity, regioselectivities, and/or substrate generality, particularly for the hydroformylation of internal olefins. On the other hand, some spiro structures have been recognized as being the privileged backbone for the construction of chiral ligands in asymmetric catalysis,[9] which have been rarely explored in the hydroformylation of olefins.[10] In the present work, we report the development of a new class of bisphosphorus ligands with a spiroketal backbone[11] and chelating units of *N*-pyrrolylphosphorus (Scheme 2), whose high π-acidity has been disclosed as a highly desirable attribute for hydroformylation of internal olefins.[6–7] The rhodium complexes of these ligands were shown to be highly efficient and regioselective in the catalytic hydroformylation of various terminal and internal olefins.

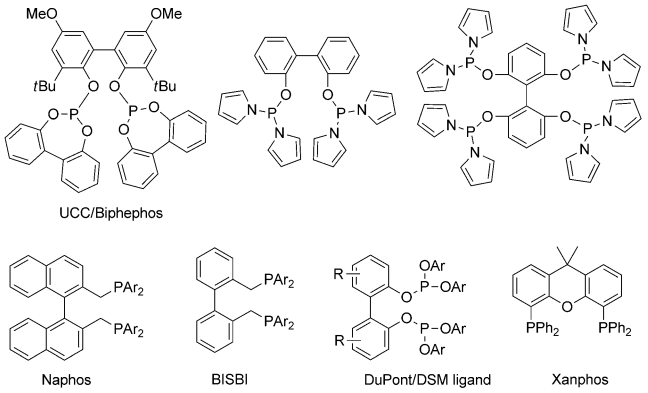

Scheme 1. Selected examples of phosphine ligands for Rh-catalyzed hydroformylation of olefins.

Results and Discussion

The spiroketal-derived bisphosphoramidite ligands **3a–i** were readily synthesized by using a four-step reaction sequence (for details, see the Supporting Information). As show in Scheme 2, the base-mediated condensation of 2,3-dimethoxyarylaldehydes and alkyl ketones afforded the bis(2,3-dimethoxybenzylidene)cyclopentanone derivatives **1** in good to excellent yields. Ni-catalyzed hydrogenation of **1**, followed by BBr_3-mediated demethylation and acetalization in one-pot, gave the key intermediate diphenols **2** as a *cis*/*trans* isomeric mixture. The desired ligands **3** were finally

[a] X. Jia, Prof. Dr. C. Xia
State Key Laboratory of Oxo Synthesis and
Selective Oxidation, Lanzhou Institute of Chemical Physics
Chinese Academy of Sciences, 18 Tianshui Middle Road
Lanzhou 730000 (P.R. China)
E-mail: cgxia@lzb.ac.cn

[b] X. Jia, Dr. Z. Wang, Prof. Dr. K. Ding
State Key Laboratory of Organometallic Chemistry
Shanghai Institute of Organic Chemistry
Chinese Academy of Sciences, 345 Lingling Road
Shanghai 200032 (P.R. China)
Fax: (+86) 21-6416-6128
E-mail: kding@mail.sioc.ac.cn

Supporting information for this article is available on the WWW under http://dx.doi.org/10.1002/chem.201203042.

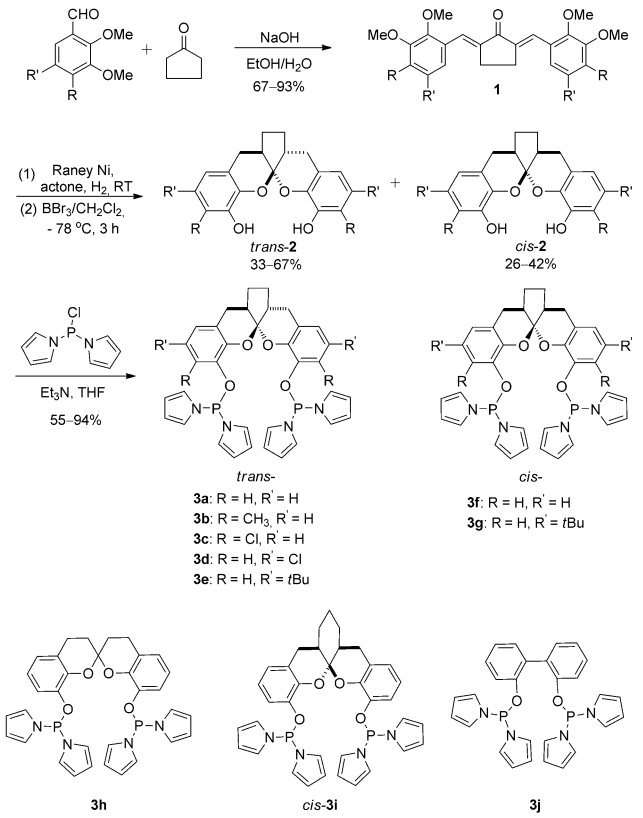

Scheme 2. Synthesis of bisphosphoramidite ligands **3a–i**.

prepared by treatment of diphenols **2** with chlorodipyrolyphosphine in the presence of Et_3N as a HCl scavenger. These ligands are stable enough in the air, and were purified by column chromatography on silica gel without special precaution to water or air.

The Rh^I-catalyzed hydroformylation of terminal olefins was first studied with spiroketal-based phosphorus ligand **3a** as the ligand and 1-hexene as the model substrate. The catalyst was prepared in situ by mixing $[Rh(acac)(CO)_2]$ with ligand **3a** at the specified molar ratios, and the reactions were carried out in toluene. For a preliminary screening of reaction conditions, a substrate/catalyst (S/C) ratio of 10000 was used. The effects of the ligand/metal ratio, reaction temperature, as well as the partial pressures of CO/H_2 were examined, and the results are summarized in Table 1. Under otherwise identical conditions, increasing the **3a**/Rh^I ratio from 1:1 to 2:1 resulted in a considerable enhancement of the regioselectivity towards the linear aldehyde (*l/b* ratio from 21.9 to 146.1, Table 1, entry 2 vs. 1), whereas further increment of the ligand/metal ratio did not alter the regioselectivity to a significant extent (Table 1, entries 3–4 vs. 2). As expected, the reaction temperature also displayed a significant effect on the hydroformylation. Although a higher regioselectivity and a lower percentage of alkene isomerization were observed at a relatively lower temperature (90 °C), a higher temperature (100 °C) was necessary to afford a higher reaction rate (Table 1, entry 2 vs. 5). Notably, a high regioselectivity was still achieved even under a temperature of 140 °C (*l/b* = 50.0, entry 7), attesting the thermal robustness of the catalyst system, which is a valuable attribute for industrial high-temperature hydroformylation of long-chained olefins.[12] The partial pressure of the syngas was also found to be crucial for the reaction. Decreasing the H_2/CO pressure from 20/20 to10/10 bar resulted in a higher percentage of alkene isomerization (Table 1, entry 8 vs. 2), whereas increasing the H_2/CO pressure to 30/30 bar led to an enhancement of the rate and alleviated isomerization, albeit at a cost of slightly lower regioselectivity (Table 1, entry 9). Thus, the preliminary optimal conditions (toluene, 100 °C, H_2/CO = 20/20 bar, substrate/L/Rh = 10000:2:1) were chosen for the ligand screening.

Table 1. Optimization of reaction conditions for the **3a**/$[Rh(acac)(CO)_2]$-catalyzed hydroformylation of 1-hexene.[a]

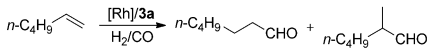

Entry	**3a**/Rh	*T* [°C]	CO/H_2 [bar]	*l/b*[b]	Linear[c] [%]	Iso[d] [%]	TON[e] [$\times 10^3$]
1	1:1	100	20/20	21.9	95.6	17.9	6.9
2	2:1	100	20/20	146.1	99.3	16.0	7.5
3	3:1	100	20/20	160.3	99.4	18.3	7.5
4	4:1	100	20/20	146.1	99.3	17.6	7.5
5	2:1	90	20/20	177.6	99.4	12.7	6.3
6	2:1	110	20/20	103.2	99.0	18.9	6.9
7	2:1	140	20/20	50.0	98.0	23.7	7.5
8	2:1	100	10/10	157.7	99.4	27.1	6.3
9	2:1	100	30/30	113.9	99.1	11.1	7.8

[a] S/C = 10000, $[Rh(acac)(CO)_2]$ (0.001 mmol), toluene (1.0 mL) as solvent, decane as the internal standard, reaction time = 3 h. [b] Linear/branched ratio, determined by GC analysis. [c] Percentage of linear aldehyde in all aldehydes. [d] Isomerization to 2-hexenes. [e] Turnover number, determined by GC analysis.

Subsequently, ligands **3b–j** were tested for Rh-catalyzed hydroformylation of 1-hexene under the reaction conditions optimized above for ligand **3a**. The results are shown in Table 2. In comparison with **3a**, ligand **3b** with an *ortho*-methyl substituent gave a substantially lower *l/b* ratio and a declined reaction rate, whereas **3c** with an *ortho*-chlorine on

Table 2. Ligand screening for hydroformylation of 1-hexene.[a]

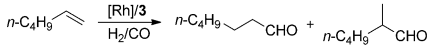

Entry	Ligand	*l/b*[b]	Linear[c] [%]	Iso[d] [%]	TON[e] [$\times 10^3$]
1	**3a**	146.1	99.3	16.0	7.5
2	**3b**	4.9	83.1	2.4	3.3
3	**3c**	146.1	99.3	19.6	6.6
4	**3d**	174.4	99.4	18.0	7.8
5[f]	**3d**	207.3	99.5	17.7	5.7
6	**3e**	122.5	99.2	8.2	7.2
7	**3f**	5.2	83.8	8.5	3.6
8	**3g**	5.5	84.6	3.3	3.9
9	**3h**	6.1	85.8	16.3	6.6
10	**3i**	2.2	68.5	9.2	7.8
11	**3j**	86.7	98.9	8.7	9.0

[a] S/C = 10000, $[Rh(acac)(CO)_2]$ (0.001 mmol), ligand/Rh ratio = 2:1, *T* = 100 °C, CO/H_2 = 20/20 bar, 3 h. toluene (1.0 mL) as solvent, decane as the internal standard. [b–e] See Table 1. [f] Reaction time: 1 h.

the phenyl rings of the ligand backbone afforded an overall similar catalytic performance. The use of ligand **3d**, bearing a chlorine substituent for R′ on the phenyl groups of the spiro backbone, resulted in an enhancement of the regioselectivity (*l*/*b* = 174.4, Table 2, entry 4). In the initial stage of the reaction (1 h), the TON value for the catalysis using this ligand was determined to be quite high (5.7×10^3, Table 2, entry 5). Ligand **3e** with bulky *t*Bu groups for R′ substituents resulted in a diminished percentage of isomerization (Table 2, entry 6 vs. 1). On the other hand, the *cis*-configured ligands **3f**, **3g**, and **3i** consistently afforded results that were inferior to their *trans*-isomers in terms of both activity and regioselectivity (Table 2, entries 7 vs. 1, 8 vs. 6, and entry 10, respectively), indicating that a subtle modification of the ligand structure in **3** can lead to a drastic change in catalytic behavior. Additionally, ligand **3h** with an untethered 2,2′-spirobis[chroman] backbone also afforded a considerably lower *l*/*b* ratio relative to that of **3a** (Table 2, entry 9 vs. 1), albeit with comparable catalytic activity, presumably as a result of increased conformational freedom in transition states when using the Rh/**3h** catalyst. For comparison, a known ligand **3j**[6] with a biphenyl backbone was also tested in this reaction under the conditions optimized for **3a**; the ligand **3j** afforded a somewhat lower *l*/*b* ratio than that of the latter, albeit with a slightly higher activity (Table 2, entry 11 vs. 1). These results suggested that both the geometry and the rigidity of the backbone in ligand **3** are important in the Rh/**3**-catalyzed hydroformylation of 1-hexene. As a compromise between catalytic selectivity and activity, ligands **3a**, **3d**, and **3j** were used in subsequent studies on hydroformylation of terminal olefins.

Under the optimized reaction conditions, a variety of terminal olefins were investigated as substrates for Rh/**3** catalyzed hydroformylation. As shown in Table 3, the short-chain olefins such as propylene and 1-butylene are readily amenable to the hydroformylation procedure, affording excellent linear/branched ratios in the catalysis (*l*/*b* = 53.3–106.5, entries 1, 2, 4, and 5). Ligand **3d** tends to be slightly more active than **3a**, and both attained a high regioselectivity in these reactions. In the cases of longer chain substrates 1-hexene and 1-octene, the regioselectivities towards the linear aldehyde products were also high (*l*/*b* = 58.2–174.4, Table 3, entries 7, 8, 10, 11), though some isomerization products could be found. For comparison, hydroformylation of these terminal olefins were also conducted with **3j** as the ligand (Table 3, entries 3, 6, 9, and 12). Under the otherwise identical conditions, ligands **3a** and **3d** consistently afforded higher *l*/*b* values than **3j** with a biphenyl backbone, thus attesting the advantages of spiroketal backbone in this type of ligands. Remarkably, for the hydroformylation of styrene, an olefin well-known to favor the formation of the branched aldehyde in many Rh-catalyzed hydroformylation studies,[13] both **3d** and **3j** afforded preferentially the linear aldehyde with a moderate selectivity (Table 3, entries 13–14).

Table 3. Hydroformylation of terminal olefins.[a]

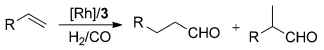

Entry	Substrate	L	CO/H_2 [bar]	*l*/*b*[b]	Linear[c] [%]	Iso.[d] [%]	TON[e]
1[f]	propylene	**3a**	10/10	53.6	98.2	–	1.4×10^4
2[f]	propylene	**3d**	10/10	58.2	98.3	–	2.1×10^4
3[f]	propylene	**3j**	10/10	23.3	95.9	–	4.8×10^4
4[g]	1-butylene	**3a**	10/10	97.0	99.0	–	1.6×10^4
5[g]	1-butylene	**3d**	10/10	106.5	99.1	–	2.3×10^4
6[g]	1-butylene	**3j**	10/10	53.3	98.2	–	4.5×10^4
7	1-hexene	**3a**	20/20	146.1	99.3	16.0	7.5×10^3
8	1-hexene	**3d**	20/20	174.4	99.4	18.0	7.8×10^3
9	1-hexene	**3j**	20/20	86.7	98.9	8.7	9.0×10^3
10	1-octene	**3a**	20/20	59.2	98.3	19.9	6.9×10^3
11	1-octene	**3d**	20/20	58.2	98.3	22.6	7.5×10^3
12	1-octene	**3j**	20/20	39.8	97.6	12.9	8.7×10^3
13	styrene	**3d**	5/5	3.4	77.5	–	6.0×10^3
14	styrene	**3j**	5/5	3.5	78.0	–	6.9×10^3

[a] S/C = 10000, $[Rh(acac)(CO)_2]$ (0.001 mmol), ligand/Rh ratio = 2:1, T = 100 °C, 3 h. toluene (1.0 mL) as solvent, decane as internal standard. [b–e] See Table 1. [f] S/C = 50000, toluene (2.0 mL) as solvent. [g] S/C = 50000.

Encouraged by these results, the isomerization–hydroformylation of more challenging internal olefins was then investigated using the industrially important (*E*)-2-butylene as the standard substrate in the presence of **3**/Rh (S/C = 50000) as the catalyst. The effects of ligand/metal ratio, temperature, and pressure on the regioselectivity and catalytic activity were evaluated, and the results are summarized in Table 4. For the reactions involving ligand **3a**, the regioselectivity for the linear aldehyde increased with the increment of **3a**/Rh ratio from 1:1 to 3:1 (Table 4, entries 1–3), whereas further increasing the ratio to 4:1 resulted in a decline in catalytic activity (entry 4). The CO/H_2 partial pressure was also found to influence the reaction (Table 4, entries 5–7). Raising the H_2 pressure led to an enhancement of

Table 4. Hydroformylation of (*E*)-2-butylene under different reaction conditions.[a]

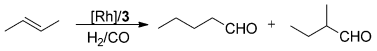

Entry	L	L/Rh	CO/H_2 [bar]	T [°C]	*l*/*b*[b]	Linear[c] [%]	TON[d]
1	**3a**	1:1	5/10	110	15.7	94.0	6.9×10^3
2	**3a**	2:1	5/10	110	26.7	96.4	6.6×10^3
3	**3a**	3:1	5/10	110	28.5	96.6	6.8×10^3
4	**3a**	4:1	5/10	110	24.1	96.0	5.4×10^3
5	**3a**	3:1	5/5	110	19.1	95.0	6.8×10^3
6	**3a**	3:1	5/15	110	27.6	96.5	7.2×10^3
7	**3a**	3:1	10/10	110	16.4	94.3	3.5×10^3
8	**3a**	3:1	5/10	100	34.5	97.2	3.8×10^3
9	**3a**	3:1	5/10	120	18.7	94.9	6.9×10^3
10	**3c**	3:1	5/10	110	27.3	96.5	6.0×10^3
11	**3d**	3:1	5/10	110	26.6	96.4	1.1×10^4
12	**3e**	3:1	5/10	110	21.0	95.5	4.2×10^3
13	**3j**	3:1	5/10	110	16.2	94.2	2.1×10^4

[a] S/C = 50000, $[Rh(acac)(CO)_2]$ (0.001 mmol), 15 h, toluene (1.0 mL) as solvent, decane as internal standard. [b–d] See Table 1.

both regioselectivity and activity (Table 4, entry 6 vs. 5), whereas increasing the CO pressure resulted in a reverse effect (Table 4, entry 7 vs. 3). With the temperature ranging from 100 to 120 °C, the regioselectivity increased with the lowering of reaction temperature, but the reaction rate exhibited a reverse trend (Table 4, entries 8, 9 vs. 3). As a compromise, the temperature of 110 °C was thus chosen for subsequent studies. Ligands **3c**–**3e** were also examined in this reaction under the conditions optimized for **3a**, affording generally high regioselectivities for the linear aldehyde (l/b = 21.0-27.3, Table 4, entries 10–12). As compared to the ligand **3a**, ligand **3c** with a chlorine for R (*o*-Cl on the aryl ring) delivered lower catalytic activity (Table 4, entry 10 vs. 3), whereas **3d** with a chlorine for R′ (*m*-Cl on the aryl ring) improved the TON value from 6.8×10^3 to 1.1×10^4 (Table 4, entry 11 vs. 3). Ligand **3e** with electron-donating *t*Bu groups for R′ also resulted in a significant degradation in catalytic activity (Table 4, entry12 vs. 3). As a comparison, ligand **3j** was also tested in this reaction, affording an inferior regioselectivity to that of **3a**, albeit with a somewhat higher activity (Table 4, entry 13 vs. 3).

Finally, the isomerization–hydroformylation of some internal olefins, including (*Z*)-2-butylene, 2-butylene isomeric mixture (*E*/*Z* = 1/1), 2-octene (*Z*/*E* = 4/1), was conducted under the optimized reaction conditions (110 °C, CO/H_2 = 5/10 bar) using **3**/Rh (L/Rh = 3, S/C = 50000) as the catalyst, and the results are shown in Table 5. With either **3a** or **3d** as the ligand, the reaction of (*Z*)-2-butylene proceeded much faster than that of its (*E*)-isomer under the otherwise identical conditions, and slightly higher regioselectivity was achieved in the reaction of (*Z*)-2-butylene (Table 5, entries 1, 2 vs. 4, 5, respectively). Such a difference in reactivity between (*Z*)- and (*E*)-2-butylene probably reflects their steric interaction with the catalyst during the olefin coordination and/or insertion into the Rh–H bond, as a result of the distinct geometrical arrangement of methyl groups around the olefin double bond. A 1:1 (*Z*/*E*)-mixture of 2-butylene was also examined in the Rh-catalyzed isomerization–hydroformylation reaction using either **3a** or **3d** as the ligand, affording excellent l/b ratios and high TON values that are approximately a statistical average of those obtained using the two isolated isomers, respectively (Table 5, entries 7–8). In the case of longer-chain substrate 2-octene (*Z*/*E* = 4/1), the regioselectivities towards the linear aldehyde were also high for both Rh/**3a** and Rh/**3d** catalysts (l/b = 23.4 and 24.0, Table 5, entries 10, 11). Under otherwise identical conditions, hydroformylation of these internal olfins with the biphenol-based ligand **3j** always afforded a lower regioselectivity than those of **3a** and **3d**, albeit with a higher activity (Table 5, entries 3, 6, 9, and 12).

Table 5. Hydroformylation of internal olefins.[a]

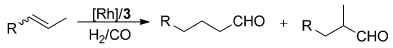

Entry	Substrate	L	l/b[b]	Linear[c] [%]	TON[d]
1	(*Z*)-2-butylene	**3a**	31.8	97.0	1.2×10^4
2	(*Z*)-2-butylene	**3d**	30.6	96.8	2.0×10^4
3	(*Z*)-2-butylene	**3j**	18.2	94.8	2.7×10^4
4	(*E*)-2-butylene	**3a**	28.5	96.6	6.8×10^3
5	(*E*)-2-butylene	**3d**	26.6	96.4	1.1×10^4
6	(*E*)-2-butylene	**3j**	16.2	94.2	2.1×10^4
7	2-butylene	**3a**	29.4	96.7	8.9×10^3
8	2-butylene	**3d**	27.8	96.5	1.5×10^4
9	2-butylene	**3j**	20.0	95.2	2.1×10^4
10[e]	2-octene	**3a**	23.4	95.9	3.8×10^3
11[e]	2-octene	**3d**	24.0	96.0	4.5×10^3
12[e]	2-octene	**3j**	19.2	95.1	6.6×10^3

[a] S/C = 50000, $[Rh(acac)(CO)_2]$ (0.001 mmol), ligand/Rh ratio = 3:1, T = 110 °C, 15 h. toluene (1.0 mL) as solvent, decane as internal standard. [b–d] See Table 1. [e] S/C = 10000.

The precatalyst with the formula [Rh(**3d**)(acac)] has been characterized by X-ray crystallography. As shown in Figure 1 a, the Rh center of the complex adopts a square-planar coordination with the chelating **3d** and acac ligands, indicating that despite the steric bulkiness of the spiro-bisphosphoramidite ligand, *cis* coordination in the complex is still feasible. The P-Rh-P bite angle (94.7°) and Rh–P bond lengths (2.161 and 2.165 Å) are similar to those found in [Rh(acac)] complexes containing bidentate phosphite ligands[14] or monodentate *N*-pyrrolylphosphines.[15] The spiroketal backbone forms a twelve-membered heterometallocyclic ring with the Rh center, and thus enforcing sufficient steric hindrance of the pyrrolyl rings around the rhodium center. Additionally, the catalytically active hydride complex $[HRh(CO)_2(\mathbf{3d})]$ was prepared in C_6D_6 under hydroformylation conditions and was characterized by ^1H- and ^{31}P NMR, as well as IR spectroscopic analyses (for details, see the Sup-

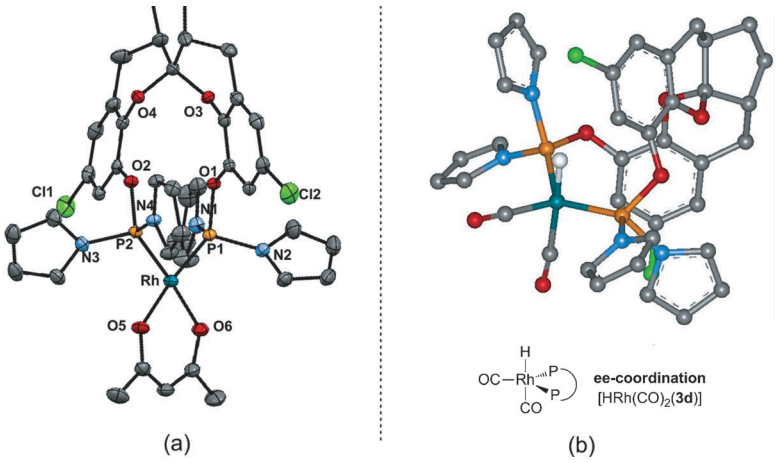

Figure 1. Crystal structure of a) [Rh(**3d**)(acac)] and b) schematic representations of the bisequatorially coordinated hydride complex $[HRh(CO)_2(\mathbf{3d})]$.

Table 6. Spectroscopic data of the [HRh(CO)$_2$**3**] complex.[a]

Complex	$\delta(^1H)$ [ppm]	$\delta(^{31}P)$ [ppm]	J_{HP} [Hz]	J_{HRh} [Hz]	J_{RhP} [Hz]	ν_{CO} [cm^{-1}]
[HRh(CO)$_2$(**3d**)]	−10.1 (br)	135	n.d.	n.d	220	2073, 2027
[HRh(CO)$_2$(**3j**)][b]	−10.7 (br)	138	n.d.	n.d.	218	2078, 2026

[a] Measured in [D$_6$]benzene. [b] See ref. [6]. n.d = not determined.

porting Information). As shown in Table 6, the key spectral data measured for the complex [HRh(CO)$_2$(**3d**)] are quite similar to those for [HRh(CO)$_2$(**3j**)], which has been reported by van Leeuwen[6] to adopt a trigonal bipyramidal structure wherein the bidentate ligand coordinates in a bis-equatorial (eq–eq) fashion to Rh^I (Figure 1b). The IR spectrum of [HRh(CO)$_2$(**3d**)] displayed two absorption bands for the carbonyl ligands around 2073 and 2027 cm^{-1}, typical for those eq–eq-coordinated [HRh(CO)$_2$(L-L)] complexes. In view of these facts, it may be concluded that for the catalytically active hydride complexes only the eq–eq-coordinated [HRh(CO)$_2$(**3d**)] isomer is present in the present reaction system (Figure 1b). Such a ligating pattern coupled with the steric hindrance of the pyrrolyl rings around the rhodium center, might account for the high regioselectivities observed in Rh/**3d** catalysis.

Conclusion

A new class of bidentate phosphoramidite ligands, based on a spiroketal backbone, has been developed for the rhodium-catalyzed hydroformylation reactions. A range of short- and long-chain olefins, including both terminal and internal olefins, were found amenable to the protocol, affording high catalytic activity and excellent regioselectivity for the linear aldehydes. A comparative study also indicated that the spiroketal is superior to the biphenyl as the backbone of the ligand in terms of the regioselectivity of the hydroformylation reactions. X-ray crystallographic analysis revealed a *cis* coordination of the ligand in the precatalyst [Rh(**3d**)(acac)], whereas NMR and IR studies on the catalytically active hydride complex [HRh(CO)$_2$(**3d**)] suggested a eq–eq coordination of the ligand in the species. We believe that the facile synthesis and excellent catalytic performance of the ligands will stimulate further research on the application of spiro-backbone-based ligands in industrially important hydroformylation reactions.

Experimental Section

General methods: Unless otherwise noted, all manipulations involving air- or moisture-sensitive compounds were performed in a nitrogen-filled glovebox or by using standard Schlenk techniques. Solvents were dried according to standard procedures. Melting points were measured on a RY-I apparatus and are uncorrected. ^{1}H, ^{13}C, and ^{31}P NMR spectra were recorded on a Varian Mercury 300 MHz or 400 MHz spectrometer. Chemical shifts (δ values) were reported in ppm with internal TMS (^{1}H NMR), $CDCl_3$ (^{13}C NMR), or external 85% H_3PO_4 (^{31}P NMR), respectively. EI (70 eV) and ESI mass spectra were obtained on HP5989 A and Mariner LC-TOF spectrometers, respectively. HRMS (EI) and HRMS (ESI) were determined on Waters Micromass GCT Premier and APEX III 7.0 TESLA FTMS spectrometers. Elemental analyses (C, H, N) were performed with an Elemental VARIO EL apparatus. The IR spectra were measured on a NICOLET AVATAR 330 or a Bruker Tensor 27 spectrometer. GC analyses were measured on an Agilent 6890N or an Agilent 7820 A system.

A general procedure for preparation of ligand 3: A solution of diol (0.32 mmol) in THF was added dropwise to a solution of 1,1′-(chlorophosphinediyl)bis(1*H*-pyrrole) (190.6 mg, 0.96 mmol) and triethylamine (0.26 mL, 1.92 mmol) in THF (1 mL) at 0 °C. After stirring at room temperature for 5 h, the precipitated $Et_3N{\cdot}HCl$ salt was filtered off, and the solvent of the filtrate was removed under vacuum. The residue was purified by flash column chromatography on silica gel (PE/EA = 10/1) to afford the product ligand **3**.

Ligand 3a: White solid, 94% yield. M.p. 115 °C; ^{1}H NMR ($CDCl_3$, 400 MHz): δ = 6.92–6.84 (m, 4H), 6.77–6.76 (m, 6H), 6.68–6.66 (m, 4H), 6.17–6.15 (m, 8H), 2.89 (dd, J = 16.0, 6.8 Hz, 2H), 2.53 (dd, J = 16.0, 7.6 Hz, 2H), 2.33–2.29 (m, 2H), 1.91–1.88 (m, 2H), 1.44–1.41 (m, 2H) ppm. ^{13}C NMR ($CDCl_3$, 100 MHz): δ = 144.0 (d, J = 2.2 Hz), 143.99 (d, J = 1.5 Hz), 141.9 (d, J = 5.2 Hz), 141.8 (d, J = 5.2 Hz), 125.9, 124.5, 121.8, 121.3 (d, J = 4.5 Hz), 121.2 (d, J = 3.7 Hz), 121.1 (d, J = 3.7 Hz), 119.4 (d, J = 3.0 Hz), 119.3 (d, J = 3.7 Hz), 111.97 (d, J = 2.2 Hz), 111.95 (d, J = 2.2 Hz), 111.82 (d, J = 2.3 Hz), 111.80 (d, J = 2.2 Hz), 109.5, 41.4, 27.8, 27.8 ppm; ^{31}P NMR (161 MHz, $CDCl_3$): δ = 111.4 ppm; FTIR (neat): 2953, 2928, 2864, 1586, 1467, 1453, 1258, 1177, 1054, 1035, 726 cm^{-1}; ESI-MS: m/z: 635; HRMS (ESI) m/z: calcd for $C_{35}H_{32}N_4NaO_4P_2^+$: 657.1791 [$M$+Na$^+$]; found: 657.1781.

Ligand 3b: White solid, 92% yield. M.p. 142 °C; ^{1}H NMR ($CDCl_3$, 400 MHz): δ = 6.78–6.74 (m, 12H), 6.20 (t, J = 2.4 Hz, 4H), 6.11 (t, J = 1.6 Hz, 4H), 2.75 (dd, J = 15.6, 6.4 Hz, 2H), 2.45 (dd, J = 15.6, 7.2 Hz, 2H), 2.25–2.17 (m, 2H), 1.93 (s, 6H), 1.85–1.84 (m, 2H), 1.39–1.38 (m, 2H) ppm; ^{13}C NMR ($CDCl_3$, 100 MHz): δ = 143.8 (d, J = 2.3 Hz), 143.7 (d, J = 2.2 Hz), 140.5 (d, J = 4.4 Hz), 128.9 (d, J = 1.5 Hz), 128.85, 123.8, 123.2, 122.7, 121.4, 121.37 (d, J = 2.3 Hz), 121.29 (d, J = 2.3 Hz), 121.2, 111.77 (d, J = 2.3 Hz), 111.75 (d, J = 2.2 Hz), 111.6 (d, J = 2.2 Hz), 111.58 (d, J = 2.2 Hz), 109.8, 41.2, 27.6, 27.5, 15.9 ppm. ^{31}P NMR (161 MHz, $CDCl_3$): 112.0 ppm; FTIR (neat): 2964, 2930, 1576, 1494, 1454, 1177, 1069, 1052, 1034, 990, 728 cm^{-1}; ESI-MS: m/z: 663 [M+H$^+$]; HRMS (ESI): m/z: calcd for $C_{37}H_{36}N_4NaO_4P_2^+$: 685.2104 [$M$+Na$^+$]; found: 685.2099.

Ligand 3c: Colorless liquid, 67% yield. ^{1}H NMR ($CDCl_3$, 400 MHz): δ = 6.96 (d, J = 8.4 Hz, 2H), 6.78–6.66 (m, 10H), 6.21–6.20 (m, 8H), 3.03 (dd, J = 16.8, 6.8 Hz, 2H), 2.52 (dd, J = 16.8, 7.2 Hz, 2H), 2.30–2.26 (m, 2H), 1.97–1.94 (m, 2H), 1.44–1.43 (m, 2H) ppm; ^{13}C NMR ($CDCl_3$, 100 MHz): δ = 144.83 (d, J = 2.0 Hz), 144.81 (d, J = 2.1 Hz), 140.87 (d, J = 5.3 Hz), 140.82 (d, J = 4.1 Hz), 129.0, 124.1, 122.4, 121.2, 121.14, 121.07, 120.98, 119.76 (d, J = 3.3 Hz), 119.73 (d, J = 3.3 Hz), 112.26 (d, J = 2.1 Hz), 112.24 (d, J = 2.4 Hz), 112.11 (d, J = 2.5 Hz), 112.08 (d, J = 2.5 Hz), 109.0, 40.6, 28.0, 25.7 ppm; ^{31}P NMR (161 MHz, $CDCl_3$): δ = 108.8 ppm; FTIR (neat): $\tilde{\nu}$ = 1585, 1469, 1453, 1226, 1177, 1034, 886, 728 cm^{-1}; ESI-MS: m/z: 703 [M+H$^+$]; HRMS (ESI): m/z: calcd for $C_{35}H_{31}Cl_2N_4O_4P_2^+$: 703.1192 [$M$+H$^+$]; found: 703.1177.

Ligand 3d: White solid, 50% yield. M.p. 90 °C; ^{1}H NMR ($CDCl_3$, 400 MHz): δ = 6.90 (d, J = 2.0 Hz, 2H), 6.76–6.69 (m, 10H), 6.21–6.19 (m, 8H), 2.83 (dd, J = 16.0, 6.4 Hz, 2H), 2.48 (dd, J = 15.6, 7.2 Hz, 2H), 2.30–2.26 (m, 2H), 1.93–1.90 (m, 2H), 1.42–1.39 (m, 2H) ppm; ^{13}C NMR ($CDCl_3$, 75 MHz): δ = 142.61 (d, J = 1.7 Hz), 142.58 (d, J = 1.7 Hz), 142.3 (d, J = 5.2 Hz), 142.2 (d, J = 5.7 Hz), 127.1, 126.4, 124.3, 121.2 (d, J = 3.5 Hz), 121.1 (d, J = 2.9 Hz), 121.0 (d, J = 2.9 Hz), 119.7 (d, J = 3.4 Hz), 119.6 (d, J = 3.5 Hz), 112.32 (d, J = 2.3 Hz), 112.30 (d, J = 2.3 Hz), 112.19 (d, J = 2.2 Hz), 112.16 (d, J = 2.3 Hz), 109.8, 41.3, 27.8, 27.6 ppm; ^{31}P NMR (161 MHz, $CDCl_3$): δ = 111.8 ppm; FTIR (neat): $\tilde{\nu}$ = 2962, 2941, 2873, 1584, 1469, 1451, 1426, 1189, 1177, 1053, 1034, 1012, 999, 729 cm^{-1};

ESI-MS: *m/z*: 703 [*M*+H$^+$]; HRMS (ESI): *m/z*: calcd for $C_{35}H_{31}Cl_2N_4O_4P_2^+$: 703.1192 [*M*+H$^+$]; found: 703.1178.

Ligand 3e: White solid, 95% yield. M.p. 164°C; ^{1}H NMR ($CDCl_3$, 400 MHz): δ=6.92 (d, *J*=2.0 Hz, 2H), 6.80–6.78 (m, 4H), 6.74 (d, *J*=2.4 Hz, 2H), 6.68–6.66 (m, 4H), 6.17 (dt, *J*=10.0, 2.0 Hz, 8H), 2.85 (dd, *J*=16.0, 6.8 Hz, 2H), 2.51 (dd, *J*=15.6, 7.2 Hz, 2H), 2.28–2.24 (m, 2H), 1.89–1.86 (m, 2H), 1.44–1.40 (m, 2H), 1.27 (s, 18H) ppm; ^{13}C NMR ($CDCl_3$, 100 MHz): δ=145.0, 141.48 (d, *J*=2.2 Hz), 141.47 (d, *J*=2.5 Hz), 141.25 (d, *J*=5.2 Hz), 141.2, 125.0, 121.4, 121.32 (d, *J*=3.0 Hz), 121.25, 121.2, 116.52 (d, *J*=3.7 Hz), 116.48 (d, *J*=3.0 Hz), 111.86 (d, *J*=1.5 Hz), 111.84 (d, *J*=2.2 Hz), 111.63 (d, *J*=2.2 Hz), 111.61 (d, *J*=2.3 Hz), 109.5, 41.4, 34.2, 31.4, 28.1, 27.8 ppm; ^{31}P NMR (161 MHz, $CDCl_3$): 111.2 ppm; FTIR (neat): $\tilde{\nu}$=2962, 2906, 2868, 1584, 1482, 1452, 1421, 1177, 1053, 1033, 726 cm^{-1}. ESI-MS: *m/z*: 747 [*M*+H$^+$]; HRMS (ESI): *m/z*: calcd for $C_{43}H_{49}N_4O_4P_2^+$: 747.3224 [*M*+H$^+$]; found: 747.3196.

Ligand 3f: White solid, 77% yield, M.p. 112°C; ^{1}H NMR ($CDCl_3$, 300 MHz): δ=6.88–6.74 (m, 13H), 6.61 (d, *J*=8.1 Hz, 1H), 6.27–6.16 (m, 8H), 2.87 (dd, *J*=17.4, 6.6 Hz, 1H), 2.72–2.52 (m, 4H), 2.28–2.22 (m, 1H), 1.98–1.93 (m, 2H), 1.53–1.38 (m, 2H) ppm. ^{13}C NMR ($CDCl_3$, 75 MHz): δ=144.6 (d, *J*=3.4 Hz), 143.0 (d, *J*=3.4 Hz), 142.1 (d, *J*=9.8 Hz), 141.3 (d, *J*=9.1 Hz), 126.3 (d, *J*=2.2 Hz), 126.0 (d, *J*=2.3 Hz), 125.1(d, *J*=1.1 Hz), 122.3 (d, *J*=1.2 Hz), 121.5 (d, *J*=1.1 Hz), 121.3 (d, *J*=2.3 Hz), 121.2 (d, *J*=1.7 Hz), 121.1 (d, *J*=1.7 Hz), 121.0 (d, *J*=1.1 Hz), 120.9 (d, *J*=1.1 Hz), 119.4 (d, *J*=6.3 Hz), 119.0 (d, *J*=6.8 Hz), 112.1 (d, *J*=4.0 Hz), 111.9 (d, *J*=2.3 Hz), 111.8 (d, *J*=2.3 Hz), 101.8, 40.7, 37.0, 26.9, 25.5, 25.0, 23.8 ppm; ^{31}P NMR (121 MHz, $CDCl_3$): 112.3 (d, *J*=10.6 Hz), 110.4 (d, *J*=9.9 Hz) ppm; FTIR (neat): $\tilde{\nu}$=2953, 2927, 1586, 1453, 1257, 1177, 1054, 1036, 726 cm^{-1}; ESI-MS: *m/z*: 635 [*M*+H$^+$]; HRMS (ESI): *m/z*: calcd for $C_{35}H_{32}N_4Na_1O_4P_2^+$: 657.1791 [*M*+Na$^+$]; found: 657.1775.

Ligand 3g: White solid, 95% yield. M.p. 162°C; ^{1}H NMR ($CDCl_3$, 400 MHz): δ=6.86–6.74 (m, 11H), 6.56 (s, 1H), 6.26–6.23 (m, 8H), 2.81 (dd, *J*=17.2, 6.8 Hz, 1H), 2.70–2.49 (m, 4H), 2.26–2.24 (m, 1H), 1.97–1.92 (m, 2H), 1.52–1.48 (m, 2H), 1.23 (s, 9H), 1.20 (s, 9H) ppm. ^{13}C NMR ($CDCl_3$, 100 MHz): δ=144.2 (d, *J*=2.2 Hz), 144.11 (d, *J*=1.5 Hz), 142.16 (d, *J*=1.5 Hz), 142.12 (dd, *J*=1.5 Hz), 141.5 (d, *J*=9.6 Hz), 140.6 (d, *J*=8.1 Hz), 140.55, 124.1 (d, *J*=1.4 Hz), 122.8 (d, *J*=1.5 Hz), 122.5 (d, *J*=1.5 Hz), 121.6, 121.5, 121.44 (d, *J*=1.5 Hz), 121.40, 121.37, 121.35, 121.33, 121.2 (d, *J*=2.9 Hz), 116.7 (d, *J*=6.0 Hz), 116.3 (d, *J*=6.7 Hz), 112.0 (d, *J*=3.0 Hz), 111.97 (d, *J*=4.4 Hz), 111.80 (d, *J*=3.7 Hz), 111.76 (d, *J*=4.5 Hz), 101.8, 40.9, 37.2, 34.1, 34.0, 31.4, 31.3, 27.2, 25.7, 25.0, 24.1 ppm; ^{31}P NMR (161 MHz, $CDCl_3$): δ=111.2 (d, *J*=14.0 Hz), 110.4 (d, *J*=14.5 Hz) ppm; FTIR (neat): $\tilde{\nu}$=2962, 2869, 1584, 1481, 1452, 1422, 1177, 1053, 1033, 727 cm^{-1}; ESI-MS (*m/z*): 747 [*M*+H$^+$]; HRMS (ESI): *m/z*: calcd for $C_{43}H_{49}N_4O_4P_2^+$: 747.3224 [*M*+H$^+$], found: 747.3194.

Ligand 3h: White solid, 64% yield, M.p. 129°C; ^{1}H NMR ($CDCl_3$, 400 MHz): δ=6.88–6.76 (m, 12H), 6.61 (d, *J*=8.0 Hz, 2H), 6.29–6.26 (m, 8H), 2.92–2.85 (m, 2H), 2.66 (dd, *J*=17.6, 5.2 Hz, 2H), 2.24–2.18 (m, 2H), 2.01 (td, *J*=13.6, 6.8 Hz, 2H) ppm; ^{13}C NMR ($CDCl_3$, 100 MHz): δ=143.54 (d, *J*=0.8 Hz), 143.51 (d, *J*=1.6 Hz), 141.43 (d, *J*=0.8 Hz), 141.3, 125.5, 124.7, 121.5, 121.29 (d, *J*=3.0 Hz), 121.1, 120.8, 119.1, 119.0, 112.16 (d, *J*=0.8 Hz), 112.11 (d, *J*=0.7 Hz), 112.0 (d, *J*=0.8 Hz), 111.9 (d, *J*=1.1 Hz), 96.5, 30.7, 20.5 ppm. ^{31}P NMR (161 MHz, $CDCl_3$): 110.1 ppm; FTIR (neat): $\tilde{\nu}$=2940, 1586, 1468, 1177, 1034, 975, 931, 856, 730 cm^{-1}; ESI-MS: *m/z*: 609 [*M*+H$^+$]; HRMS (ESI): *m/z*: calcd for $C_{33}H_{30}N_4N_aN_aO_4P_2^+$: 631.1634 [*M*+Na$^+$]; found: 631.1620.

Ligand 3i: White solid, 76% yield. M.p. 117°C; ^{1}H NMR ($CDCl_3$, 300 MHz): δ=6.86–6.69 (m, 12H), 6.60–6.57 (m, 2H), 6.30–6.24 (m, 8H), 3.06 (dd, *J*=12.6, 4.8 Hz, 1H), 2.47–2.42 (m, 2H), 2.28 (d, *J*=12.6 Hz, 1H), 2.07–1.92 (m, 2H), 1.69–1.26 (m, 6H) ppm. ^{13}C NMR ($CDCl_3$, 75 MHz): δ=143.34 (d, *J*=1.1 Hz), 143.31(d, *J*=1.1 Hz), 142.35 (d, *J*=1.2 Hz), 142.31 (d, *J*=1.7 Hz), 141.31 (d, *J*=4.6 Hz), 141.2 (d, *J*=4.0 Hz), 126.0 (d, *J*=1.7 Hz), 125.4 (d, *J*=1.7 Hz), 125.3, 123.62 (d, *J*=1.7 Hz), 123.60 (d, *J*=1.2 Hz), 121.4 (d, *J*=2.3 Hz), 121.2, 121.16, 121.0, 120.9 (d, *J*=1.1 Hz), 120.7 (d, *J*=1.1 Hz), 119.0 (d, *J*=6.2 Hz), 118.9 (d, *J*=5.6 Hz), 112.1, 112.0, 111.9 (d, *J*=1.1 Hz), 111.86, 98.2, 38.3, 36.3, 29.3, 29.2, 27.0, 26.9, 24.4 ppm; ^{31}P NMR (121 MHz, $CDCl_3$): δ=110.9, 110.2 ppm; FTIR (neat): $\tilde{\nu}$=2921, 2854, 1586, 1462, 1450, 1258, 1177, 1049, 1036, 723 cm^{-1}; ESI-MS: *m/z*: 649 [*M*+H$^+$]; HRMS (ESI): *m/z*: calcd for $C_{36}H_{34}N_4NaO_4P_2^+$: 671.1947 [*M*+Na$^+$]; found: 671.1956.

Ligand 3j: White solid, 86% yield. ^{1}H NMR ($CDCl_3$, 400 MHz): δ=7.28–7.25 (m, 4H), 7.18–7.16 (m, 2H), 6.85 (d, *J*=8.0 Hz, 2H), 6.70 (s, 8H), 6.23 (s, 8H) ppm; ^{31}P NMR ($CDCl_3$, 161 MHz): δ=108.3 ppm.

Typical procedure for the hydroformylation of 1-hexene with ligand 3a: In a glove box, a glass vial with a magnetic stirring bar was charged with ligand **3a** (1.27 mg, 0.002 mmol) and [Rh(acac)(CO)$_2$] (0.26 mg, 0.001 mmol) in toluene (1.0 mL). The mixture was stirred for 5 min. 1-Hexene (1.24 mL, 10 mmol) was then added, followed by decane (97 μL, 0.5 mmol) as the internal standard. The resulting mixture was transferred to an autoclave, which was purged with nitrogen three times and subsequently charged with CO (20 bar) and H_2 (20 bar). The autoclave was then heated to 100°C (oil bath) for 3 h. The autoclave was cooled in ice water, and the gas was carefully released in a well-ventilated hood. The reaction mixture was immediately analyzed by GC to determine the turnover number (TON), percentage of isomerization, and regioselectivity (*l*/*b* ratio).

Typical procedure for the regioselective hydroformylation of (*E*)-2-butene with ligand 3a: In a glove box, an autoclave with a magnetic stirring bar was charged with ligand **3a** (1.90 mg, 0.003 mmol), [Rh(acac)(CO)$_2$] (0.26 mg, 0.001 mmol), and decane (97 μL, 0.5 mmol) as internal standard in toluene (1.0 mL). The mixture was stirred for 5 min. The autoclave was cooled to 0°C, purged with nitrogen three times, and then charged with (*E*)-2-butene (2.8 g, 50 mmol). The autoclave was charged with CO (5 bar) and H_2 (10 bar), and then heated to 110°C (oil bath) for 15 h. The autoclave was cooled in ice water, and the gas was carefully released in a well-ventilated hood. The reaction mixture was immediately analyzed by GC to determine the turnover number (TON) and regioselectivity (*l*/*b* ratio).

Acknowledgements

We thank the financial support of this work from the National Natural Science Foundation of China (grant nos. 20821002, 20923005, 20972176), the Major Basic Research Development Program of China (grant no. 2010CB833300), the Chinese Academy of Sciences, and the Science and Technology Commission of Shanghai Municipality.

[1] For reviews, see: a) *Rhodium Catalyzed Hydroformylation*, C. Claver, P. W. N. M. van Leeuwen, Kluwer Academic Publishers, Dordrecht, The Netherlands, **2000**; b) B. Breit, W. Seiche, *Synthesis* **2001**, 1–36; c) P. C. J. Kamer, P. W. N. M. van Leeuwen, J. N. H. Reek, *Acc. Chem. Res.* **2001**, *34*, 895–904; d) M. L. Claver, *Curr. Org. Chem.* **2005**, *9*, 701–718; e) F. Ungváry, *Coord. Chem. Rev.* **2005**, *249*, 2946–2961.

[2] a) C. P. Casey, G. T. Whiteker, M. G. Melville, L. M. Petrovich, J. A., Jr. Gavney, D. R. Powell, *J. Am. Chem. Soc.* **1992**, *114*, 5535–5543; b) W. A. Herrmann, R. Schmid, C. W. Kohlpaintner, T. Priermeier, *Organometallics* **1995**, *14*, 1961–1968; c) C. P. Casey, E. L. Paulsen, E. W. Beuttenmueller, B. R. Proft, L. M. Petrovich, B. A. Matter, D. R. Powell, *J. Am. Chem. Soc.* **1997**, *119*, 11817–11825; d) R. Paciello, L. Siggel, M. Röer, *Angew. Chem.* **1999**, *111*, 2045–2048; *Angew. Chem. Int. Ed.* **1999**, *38*, 1920–1923; e) V. F. Slagt, J. N. H. Reek, P. C. J. Kamer, P. W. N. M. van Leeuwen, *Angew. Chem.* **2001**, *113*, 4401–4404; *Angew. Chem. Int. Ed.* **2001**, *40*, 4271–4274; f) B. Breit, W. Seiche, *J. Am. Chem. Soc.* **2003**, *125*, 6608–6609; g) V. F. Slagt, P. W. N. M. van Leeuwen, J. N. H. Reek, *Angew. Chem.* **2003**, *115*, 5777–5781; *Angew. Chem. Int. Ed.* **2003**, *42*, 5619–5623; h) V. F. Slagt, P. C. J. Kamer, P. W. N. M. van Leeuwen, J. N. H. Reek, *J. Am. Chem. Soc.* **2004**, *126*, 1526–1536; i) B. Breit, W. Seiche, *Angew. Chem.* **2005**, *117*, 1666–1669; *Angew. Chem. Int. Ed.* **2005**, *44*, 1640–1643; j) H. Klein, R. Jackstell, M. Beller, *Chem.*

Commun. **2005**, 2283–2285; k) W. Seiche, A. Schuschkowski, B. Breit, *Adv. Synth. Catal.* **2005**, *347*, 1488–1494; l) M. Kuil, T. Soltner, P. W. N. M. van Leeuwen, J. N. H. Reek, *J. Am. Chem. Soc.* **2006**, *128*, 11344–11345; m) I. Piras, R. Jennerjahn, R. Jackstell, W. Baumann, A. Spannenberg, R. Franke, K.-D. Wiese, M. Beller, *J. Organomet. Chem.* **2010**, *695*, 479–486; n) P. Dydio, W. I. Dzik, M. Lutz, B. de Bruin, J. N. H. Reek, *Angew. Chem.* **2011**, *123*, 416–420; *Angew. Chem. Int. Ed.* **2011**, *50*, 396–400.

[3] H. Klein, R. Jackstell, K.-D. Wiese, C. Borgmann, M. Beller, *Angew. Chem.* **2001**, *113*, 3505–3508; *Angew. Chem. Int. Ed.* **2001**, *40*, 3408–3411.

[4] a) E. Billig, A. G. Abatjoglou, D. R. Bryant, UCC, European Patent EP 213639, 1987; U.S. Patent 4748261, **1988**; b) G. D. Cuny, S. L. Buchwald, *J. Am. Chem. Soc.* **1993**, *115*, 2066–2068.

[5] P. M. Burke, J. M. Garner, K. A. Kreutzer, A. J. J. M. Teunissen, C. S. Snijder, C. B. Hansen, DSM/Du Pont, , PCT Int. Patent WO 97/33854, **1997**.

[6] S. C. van der Slot, J. Duran, J. Luten, P. C. J. Kamer, P. W. N. M. van Leeuwen, *Organometallics* **2002**, *21*, 3873–3883.

[7] a) Y. Yan, X. Zhang, X. Zhang, *J. Am. Chem. Soc.* **2006**, *128*, 16058–16061; b) S. Yu, Y. Chie, Z. Guan, X. Zhang, *Org. Lett.* **2008**, *10*, 3469–3472; c) S. Yu, Y. Chie, Z. Guan, Y. Zou, W. Li, X. Zhang, *Org. Lett.* **2009**, *11*, 241–244.

[8] a) M. Kranenburg, Y. E. M. van der Burgt, P. C. J. Kamer, P. W. N. M. van Leeuwen, K. Goubitz, J. Fraanje, *Organometallics* **1995**, *14*, 3081–3089; b) L. A. Van der Veen, M. D. K. Boele, F. R. Bregman, P. C. J. Kamer, P. W. N. M. van Leeuwen, K. Goubitz, J. Fraanje, H. Schenk, C. Bo, *J. Am. Chem. Soc.* **1998**, *120*, 11616–11626; c) L. A. van der Veen, P. C. J. Kamer, P. W. N. M. van Leeuwen, *Angew. Chem.* **1999**, *111*, 349–351; *Angew. Chem. Int. Ed.* **1999**, *38*, 336–338; d) L. A. van der Veen, P. C. J. Kamer, P. W. N. M. van Leeuwen, *Organometallics* **1999**, *18*, 4765–4777; e) J. J. Carbó, F. Maseras, C. Bo, P. W. N. M. van Leeuwen, *J. Am. Chem. Soc.* **2001**, *123*, 7630–7637.

[9] For leading references, see: a) Y. Jiang, S. Xue, Z. Li, J. Deng, A. Mi, A. S. C. Chan, *Tetrahedron: Asymmetry* **1998**, *9*, 3185–3189; b) Y. Jiang, S. Xue, K. Yu, Z. Li, J. Deng, A. Mi, A. S. C. Chan, *J. Organomet. Chem.* **1999**, *586*, 159–165. For reviews, see; c) J.-H. Xie, Q.-L. Zhou, *Acc. Chem. Res.* **2008**, *41*, 581–593; d) G. B. Bajracharya, M. A. Arai, P. S. Koranne, T. Suzuki, S. Takizawa, H. Sasai, *Bull. Chem. Soc. Jpn.* **2009**, *82*, 285–302; e) K. Ding, Z. Han, Z. Wang, *Chem. Asian J.* **2009**, *4*, 32–41.

[10] a) Z. Freixa, M. S. Beentjes, G. D. Batema, C. B. Dieleman, G. P. F. van Strijdonck, J. N. H. Reek, P. C. J. Kamer, J. Fraanje, K. Goubitz, P. W. N. M. van Leeuwen, *Angew. Chem.* **2003**, *115*, 1322–1325; *Angew. Chem. Int. Ed.* **2003**, *42*, 1284–1287. For examples of Rh^{I}-catalyzed asymmetric hydroformylation using chiral spiro ligands, see ref. [9a] and [9b]. For an example using an elegant supramolecular approach in the construction of spiro-type wide-bite-angle diphosphine ligands in catalytic hydroformylation, see: b) D. Rivillo, H. Gulyás, J. BenetBuchholz, E. C. Escudero-Adán, Z. Freixa, P. W. N. M. van Leeuwen, *Angew. Chem.* **2007**, *119*, 7385–7388; *Angew. Chem. Int. Ed.* **2007**, *46*, 7247–7250.

[11] For the synthesis and application of spiroketal-based ligands in catalysis, see: a) P. W. N. M. van Leeuwen, M. A. Zuideveld, B. H. G. Swennenhuis, Z. Freixa, P. C. J. Kamer, K. Goubitz, J. Fraanje, M. Lutz, A. L. Spek, *J. Am. Chem. Soc.* **2003**, *125*, 5523–5539; b) Z. Freixa, P. C. J. Kamer, M. Lutz, A. L. Spek, P. W. N. M. van Leeuwen, *Angew. Chem.* **2005**, *117*, 4459–4462; *Angew. Chem. Int. Ed.* **2005**, *44*, 4385–4388; c) C. Jiménez-Rodríguez, F. X. Roca, C. Bo, J. BenetBuchholz, E. C. Escudero-Adán, Z. Freixa, P. W. N. M. van Leeuwen, *Dalton Trans.* **2006**, 268–278; d) X. Sala, E. J. G. Suárez, Z. Freixa, J. BenetBuchholz, P. W. N. M. van Leeuwen, *Eur. J. Org. Chem.* **2008**, 6197–6205; e) M. J.-L. Tschan, J.-M. López-Valbuena, Z. Freixa, H. Launay, H. Hagen, J. BenetBuchholz, P. W. N. M. van Leeuwen, *Organometallics* **2011**, *30*, 792–799; f) O. Jacquet, N. D. Clément, Z. Freixa, A. Ruiz, C. Claver, P. W. N. M. van Leeuwen, *Tetrahedron: Asymmetry* **2011**, *22*, 1490–1498; g) J. Li, G. Chen, Z. Wang, R. Zhang, X. Zhang, K. Ding, *Chem. Sci.* **2011**, *2*, 1141–1144; h) J. Li, W. Pan, Z. Wang, X. Zhang, K. Ding, *Adv. Synth. Catal.* **2012**, *354*, 1980–1986; i) X. Wang, Z. Han, Z. Wang, K. Ding, *Angew. Chem.* **2012**, *124*, 960–964; *Angew. Chem. Int. Ed.* **2012**, *51*, 936–940; j) X. M. Wang, F. Y. Meng, Y. Wang, Z. B. Han, Y. J. Chen, L. Liu, Z. Wang, K. Ding, *Angew. Chem.* **2012**, *124*, 9410–9416; *Angew. Chem. Int. Ed.* **2012**, *51*, 9276–9282.

[12] S. Yu, X. Zhang, Y. Yan, C. Cai, L. Dai, X. Zhang, *Chem. Eur. J.* **2010**, *16*, 4938–4943.

[13] C. A. Tolman, J. W. Faller, In *Homogeneous Catalysis with Metal Phosphine Complexes* (Ed.: L. H. Pignolet), Plenum: New York, **1983**; p. 81.

[14] a) F. Agbossou, J.-F. Carpentier, C. Hatat, N. Kokel, A. Mortreux, P. Betz, R. Goddard, C. Kruger, *Organometallics* **1995**, *14*, 2480–2489; b) A. Van Rooy, P. C. J. Kamer, P. W. N. M. Van Leeuwen, K. Goubitz, J. Fraanje, N. Veldman, A. L. Spek, *Organometallics* **1996**, *15*, 835–847; c) S. P. Shum, S. D. Pastor, G. Rihs, *Inorg. Chem.* **2002**, *41*, 127–131; d) C. J. Cobley, R. D. J. Froese, J. Klosin, C. Qin, G. T. Whiteker, *Organometallics* **2007**, *26*, 2986–2999.

[15] A. M. Trzeciak, T. Głowiak, R. Grzybek, J. J. Ziółkowski, *J. Chem. Soc. Dalton Trans.* **1997**, 1831–1837.

Received: August 27, 2012
Published online: November 7, 2012

